Influence of magnetic impurities on charge transport in diffusive-normal-metal/superconductor junctions

T. Yokoyama,[1] Y. Tanaka,[1] A. A. Golubov,[2] J. Inoue,[1] and Y. Asano[3]
[1]*Department of Applied Physics, Nagoya University, Nagoya, 464-8603, Japan*
and CREST, Japan Science and Technology Corporation (JST) Nagoya, 464-8603, Japan
[2]*Faculty of Science and Technology, University of Twente, 7500 AE, Enschede, The Netherlands*
[3]*Department of Applied Physics, Hokkaido University, Sapporo, 060-8628, Japan*
(Received 28 June 2004; revised manuscript received 29 November 2004; published 9 March 2005)

Charge transport in the diffusive normal metal (DN)/insulator/*s*- and *d*-wave superconductor junctions is studied in the presence of magnetic impurities in DN in the framework of the quasiclassical Usadel equations with the generalized boundary conditions. The cases of *s*- and *d*-wave superconducting electrodes are considered. The junction conductance is calculated as a function of a bias voltage for various parameters of the DN metal, resistivity, Thouless energy, the magnetic impurity scattering rate, and the transparency of the insulating barrier between DN and a superconductor. It is shown that the proximity effect is suppressed by magnetic impurity scattering in DN for any value of the barrier transparency. In low-transparent *s*-wave junctions this leads to the suppression of the normalized zero-bias conductance. In contrast to that, in high transparent junctions zero-bias conductance is enhanced by magnetic impurity scattering. The physical origin of this effect is discussed. For the *d*-wave junctions, the dependence on the misorientation angle α between the interface normal and the crystal axis of a superconductor is studied. The zero-bias conductance peak is suppressed by the magnetic impurity scattering only for low transparent junctions with $\alpha \sim 0$. In other cases the conductance of the *d*-wave junctions does not depend on the magnetic impurity scattering due to strong suppression of the proximity effect by the midgap Andreev resonant states.

DOI: 10.1103/PhysRevB.71.094506 PACS number(s): 74.50.+r, 74.20.−z

I. INTRODUCTION

Presently, thanks to the nanofabrication technique, detailed experimental studies of the electron coherence in mesoscopic superconducting systems become possible, where the Andreev reflection[1–3] plays an important role in the low energy transport. In diffusive normal metal/superconductor (DN/S) junctions, the phase coherence between incoming electrons and Andreev reflected holes persists in DN at a mesoscopic length scale and results in strong interference effects on the probability of Andreev reflection.[4]

One of the remarkable experimental manifestations of the coherent Andreev reflection is the zero bias conductance peak (ZBCP) in DN/S junctions.[5–15] The physics of ZBCP was extensively studied theoretically using scattering matrix approach[16–21] and the quasiclassical Green's function technique.[22,25–34] Volkov, Zaitsev, and Klapwijk (VZK)[22] explained the origin of the ZBCP in DN/S junctions in the framework of the quasiclassical theory by solving the Usadel equations[23] with the Kupriyanov and Lukichev (KL) boundary condition for the Keldysh-Nambu Green's function.[24] According to the VZK theory the ZBCP is due to the enhancement of the pair amplitude in DN by the proximity effect. The influence of the magnetic impurity scattering on the bias voltage dependent conductance was also studied within this approach.[22,27,35]

Recently the VZK theory for *s*-wave superconductors was extended by Tanaka *et al.*[37] using more general boundary conditions provided by the circuit theory of Nazarov.[36] These boundary conditions treat an interface as an arbitrary connector between diffusive metals. The connector is characterized by a set of transmission coefficients ranging from a ballistic point contact to a tunnel junction. The boundary conditions coincide with the KL conditions when a connector is diffusive or transmission coefficients are low, while the BTK theory[2] is reproduced in the ballistic regime. The extended VZK theory[37,44] revealed a number of new features like a *U*-shaped gap like structure and a crossover from a zero bias conductance peak (ZBCP) to a zero bias conductance dip (ZBCD). These phenomena are relevant for the actual junctions in which the barrier transparency is not necessarily small. However, the influence of the magnetic impurity scattering in DN on the charge transport was not studied in this regime.

The generalized VZK theory was recently applied also to unconventional superconducting junctions.[43,44] The formation of the midgap Andreev resonant states (MARS) at the interface of unconventional superconductors[38–41] is naturally taken into account in this approach.[43,44] It was demonstrated that the formation of MARS in DN/*d*-wave superconductor (DN/*d*) junctions strongly competes with the proximity effect. Remarkable recent advances in experiments on tunneling in high T_C cuprates[42] stimulate an interest to the problem of an influence of the magnetic impurity scattering on a charge transport in DN/*d* junctions.

In the present paper the generalized VZK theory is applied to the study of an influence of the magnetic impurity scattering in the DN on the conductance in DN/S where S is either *s*- or *d*-wave superconductor. The parameters of the problem are the height of the insulating barrier at the DN/S interface, the resistance R_d, the magnetic impurity scattering rate γ, the Thouless energy E_{Th} in DN and the angle α be-

tween the normal to the interface and the crystal axis of *d*-wave superconductors. We shall focus on the dependence of the normalized conductance $\sigma_T(\mathrm{eV})=\sigma_S(\mathrm{eV})/\sigma_N(\mathrm{eV})$, on the bias voltage V, where $\sigma_{S(N)}(\mathrm{eV})$ are the conductances in the superconducting (normal) state. The organization of the paper is as follows. In Sec. II the detailed derivation of the expression for the normalized conductance is provided. In Sec. III the results of calculations of $\sigma_T(\mathrm{eV})$ are presented for *s*- and *d*-wave junctions separately and physical explanation of the results is given. In Sec. IV the summary of the obtained results and the conclusions are presented. In this paper we restrict ourselves to zero temperature and set $k_B=\hbar=1$. In general the zero bias conductance (ZBC), by definition, is studied in the theory and in the experiment at $\mathrm{eV}\to 0$. Thus, the ZBC defined in a standard way actually depends on temperature and has certain limit at $T\to 0$. On the other hand, we calculate ZBC in another way, we first set $T=0$, then calculate the differential resistance at $\mathrm{eV}\to 0$. We are sure that the limits $T\to 0$, $\mathrm{eV}\to 0$ are commutable for the differential resistance.

II. FORMULATION

In this section we introduce the model and the formalism. We consider a junction consisting of normal and superconducting reservoirs connected by a quasi-one-dimensional diffusive conductor (DN) with a length L much larger than the mean free path. This structure was considered in Refs. 37 and 44, while in the present paper the scattering on magnetic impurities in DN is taken into account. Similar to Ref. 37 and 44, we assume that the interface between the DN conductor and the S electrode at $x=L$ has a resistance R_b while the DN/N interface at $x=0$ has zero resistance and we apply the generalized boundary conditions of Ref. 36 to treat the interface between DN and S.

We model the insulating barrier between DN and S by the delta function $U(x)=H\delta(x-L)$, which provides the transparency of the junction $T_m=4\cos^2\phi/(4\cos^2\phi+Z^2)$, where $Z=2H/v_F$ is a dimensionless constant, ϕ is the injection angle measured from the interface normal to the junction, and v_F is Fermi velocity. The interface resistance R_b is given by

$$R_b = R_0 \frac{2}{\int_{-\pi/2}^{\pi/2} d\phi T_m \cos\phi},$$

where R_0 is Sharvin resistance $R_0^{-1}=e^2k_F^2S_c/4\pi^2$, k_F is the Fermi wave vector and S_c is the constriction area (see Fig. 1). Note that the area S_c is in general not equal to the cross-section area S_d of the normal conductor, therefore S_c/S_d is independent parameter of our theory. This allows to vary R_d/R_b independently of T_m. In real physical situation, the assumption $S_c<S_d$ means that only a part of the actual flat DN/S interface (having area S_c) is conducting, no matter is it a single conducting region or a series of such regions. These conducting regions are not constrictions in a standard sense—we do not assume the narrowing of the total cross section, but rather that only the part of the cross section is conducting.

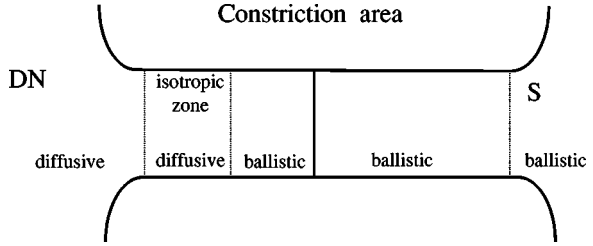

FIG. 1. Schematic illustration of the model.

We apply the quasiclassical Keldysh formalism in the following calculation of the conductance. The definitions of 4×4 Green's functions in DN and S, $\check{G}_1(x)$ and $\check{G}_2(x)$, and other notations can be found in Refs. 37 and 44. The new feature in the present model is the spin-scattering term in the static Usadel equation[23] for $\check{G}_1(x)$ in DN,

$$D\frac{\partial}{\partial x}\left(\check{G}_1(x)\frac{\partial \check{G}_1(x)}{\partial x}\right)+i[\check{H}-i\check{\Sigma}_{\mathrm{spin}},\check{G}_1(x)]=0, \qquad (1)$$

where D is the diffusion constant in DN, $\check{H}$ is given by

$$\check{H}=\begin{pmatrix}\hat{H}_0 & 0\\ 0 & \hat{H}_0\end{pmatrix},$$

with $\hat{H}_0=\epsilon\hat{\tau}_3$, and

$$\check{\Sigma}_{\mathrm{spin}}=\frac{\gamma}{2}\hat{\tau}_3\check{G}_1(x)\hat{\tau}_3$$

is the self-energy for magnetic impurity scattering with the scattering rate γ in DN. Note that magnetic impurities take random alignments and we average them in all directions, thus $\check{G}_1(x)$ in our calculation is a unit matrix in the spin space. The Nazarov's generalized boundary condition for $\check{G}_1(x)$ at the DN/S interface has the same form as the one without magnetic impurity scattering (see Refs. 37 and 44).

In the actual calculation it is convenient to use the standard θ-parametrization where $\theta(x)$ is a measure of the proximity effect in DN and is determined by the following equation:

$$D\frac{\partial^2}{\partial x^2}\theta(x)+2i\{\epsilon+i\gamma\cos[\theta(x)]\}\sin[\theta(x)]=0. \qquad (2)$$

One can see that introduction of magnetic impurity scattering γ leads to modification of the effective coherence length in DN. In particular, switching on γ makes function $\theta(x)$ exponentially decaying at zero energy, while $\theta(x)$ at $\gamma=0$ behaves linearly in DN. It will be shown below that these modifications result in suppression of θ in DN, as expected due to the pair-breaking nature of magnetic scattering, which in turn leads to corresponding modifications of the subgap conductance.

Finally, we obtain the following result for the electric current:

$$I_{el} = \frac{1}{e}\int_0^\infty d\epsilon \frac{f_{t0}}{\dfrac{R_b}{\langle I_{b0}\rangle} + \dfrac{R_d}{L}\displaystyle\int_0^L \frac{dx}{\cosh^2\theta_{im}(x)}} \tag{3}$$

with

$$f_{t0} = \tfrac{1}{2}\{\tanh[(\epsilon + eV)/(2T)] - \tanh[(\epsilon - eV)/(2T)]\}.$$

Then the total differential resistance R for s-wave junction at zero temperature is given by

$$R = \frac{R_b}{\langle I_{b0}\rangle} + \frac{R_d}{L}\int_0^L \frac{dx}{\cosh^2\theta_{im}(x)} \tag{4}$$

with

$$I_{b0} = \frac{T_m\Lambda_1 + 2(2-T_m)\Lambda_2}{2|(2-T_m) + T_m(g\cos\theta_L + f\sin\theta_L)|^2},$$

$$\Lambda_1 = (1 + |\cos\theta_L|^2 + |\sin\theta_L|^2)(|g|^2 + |f|^2 + 1) + 4\,\mathrm{Imag}(fg^*)\mathrm{Imag}(\cos\theta_L \sin\theta_L^*), \tag{5}$$

$$\Lambda_2 = \mathrm{Real}[g(\cos\theta_L + \cos\theta_L^*) + f(\sin\theta_L + \sin\theta_L^*)], \tag{6}$$

$$g = \varepsilon/\sqrt{\varepsilon^2 - \Delta^2}, \quad f = \Delta/\sqrt{\Delta^2 - \varepsilon^2}.$$

For a d-wave junction, the function I_{b0} is given by the following expression:

$$I_{b0} = \frac{T_n}{2}\frac{C_0}{|(2-T_n)(1 + g_+g_- + f_+f_-) + T_n[\cos\theta_L(g_+ + g_-) + \sin\theta_L(f_+ + f_-)]|^2}$$

$$C_0 = T_n(1 + |\cos\theta_L|^2 + |\sin\theta_L|^2)(|g_+ + g_-|^2 + |f_+ + f_-|^2 + |1 + f_+f_- + g_+g_-|^2 + |f_+g_- - g_+f_-|^2) + 2(2-T_n)$$
$$\times\mathrm{Real}\{(1 + g_+^*g_-^* + f_+^*f_-^*)[(\cos\theta_L + \cos\theta_L^*)(g_+ + g_-) + (\sin\theta_L + \sin\theta_L^*)(f_+ + f_-)]\}$$
$$+ 4T_n\mathrm{Imag}(\cos\theta_L \sin\theta_L^*)\mathrm{Imag}[(f_+ + f_-)(g_+^* + g_-^*)],$$

$g_\pm = \varepsilon/\sqrt{\varepsilon^2 - \Delta_\pm^2}$, $f_\pm = \Delta_\pm/\sqrt{\Delta_\pm^2 - \varepsilon^2}$, and $\Delta_\pm = \Delta\cos 2(\phi \mp \alpha)$. In the above α, $\theta_{im}(x)$, and θ_L denote the angle between the normal to the interface and the crystal axis of d-wave superconductors, the imaginary part of $\theta(x)$ and $\theta(L_-)$, respectively. The conductance in the superconducting state $\sigma_S(\mathrm{eV})$ is simply related to R by $\sigma_S(\mathrm{eV}) = 1/R$.

It is important to note that in the present approach, according to the circuit theory, R_d/R_b can be varied indepen-

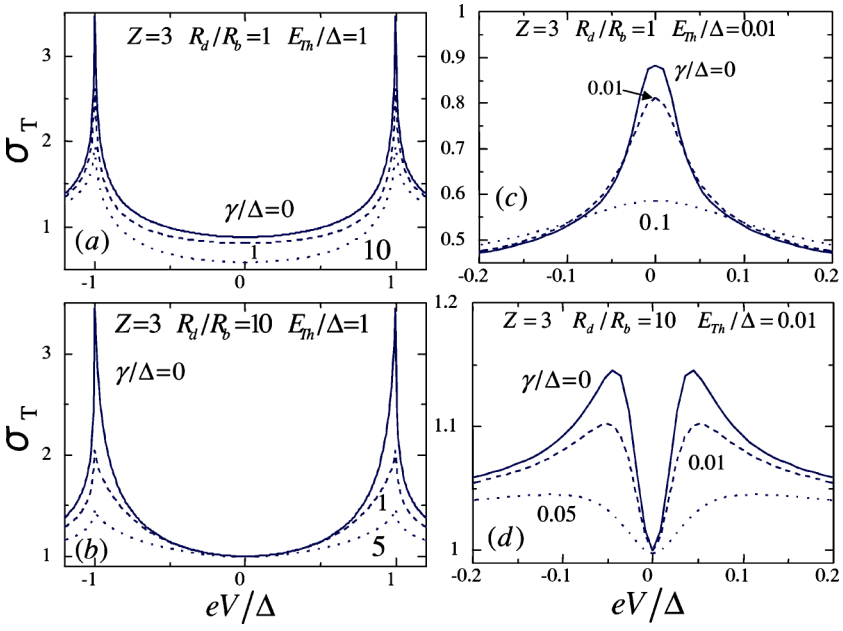

FIG. 2. Normalized conductance for $Z=3$.

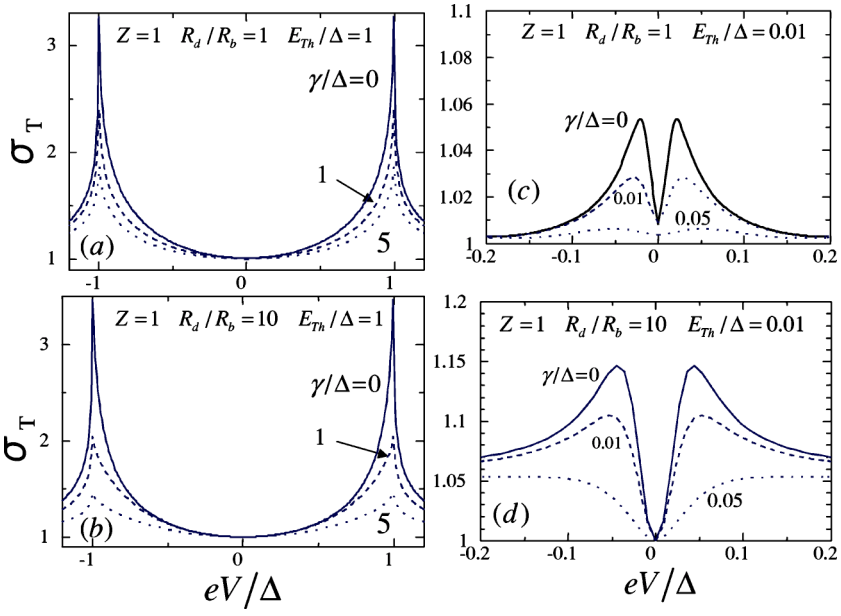

FIG. 3. Normalized conductance for $Z=1$.

dently of T_m, i.e., independently of Z, since one can change the magnitude of the constriction area S_c independently. In other words, R_d/R_b is no longer proportional to $T_{av}(L/l)$, where T_{av} is the averaged transmissivity of the barrier and l is the mean free path in the diffusive region. Based on this fact, we can choose R_d/R_b and Z as independent parameters.

In the following section, we will discuss the normalized conductance $\sigma_T(\mathrm{eV})=\sigma_S(\mathrm{eV})/\sigma_N(\mathrm{eV})$ where $\sigma_N(\mathrm{eV})$ is the conductance in the normal state without magnetic impurity given by $\sigma_N(\mathrm{eV})=\sigma_N=1/(R_d+R_b)$.

III. RESULTS

A. Tunneling conductance for *s*-wave junctions

In this section, we focus on the bias voltage dependent normalized conductance $\sigma_T(\mathrm{eV})$ for various situations. Let us first focus on the relatively low transparent junctions with $Z=3$ for various γ/Δ (Fig. 2). For $E_{\mathrm{Th}}/\Delta=1$ and $R_d/R_b=1$, the $\sigma_T(\mathrm{eV})$ curves have a rounded bottom shape and the height of the bottom value is reduced with an increase in γ/Δ. The height of the peak at $\mathrm{eV}=\pm\Delta$ is reduced with an increase in γ/Δ [see Fig. 2(a)]. For $E_{\mathrm{Th}}/\Delta=1$ and $R_d/R_b=10$, the $\sigma_T(\mathrm{eV})$ curves also have a rounded bottom structure which flattens with an increase in γ/Δ. Also the peak at $\mathrm{eV}=\pm\Delta$ is suppressed with the increase of γ/Δ [see Fig. 2(b)]. For small Thouless energy $E_{\mathrm{Th}}/\Delta=0.01$ and $R_d/R_b=1$, the conductance has a prominent ZBCP with the width given by E_{Th}. As seen from Fig. 2(c), the magnetic impurity scattering suppresses the peak height. With the increase of the resistance ratio R_d/R_b, the ZBCP transforms into ZBCD, as shown in Fig. 2(d). The magnitude of ZBCD decreases with the increase of γ/Δ, and the height of the peaks around $\mathrm{eV}/\Delta\sim 0.04$ is also reduced [see Fig. 2(d)]. As

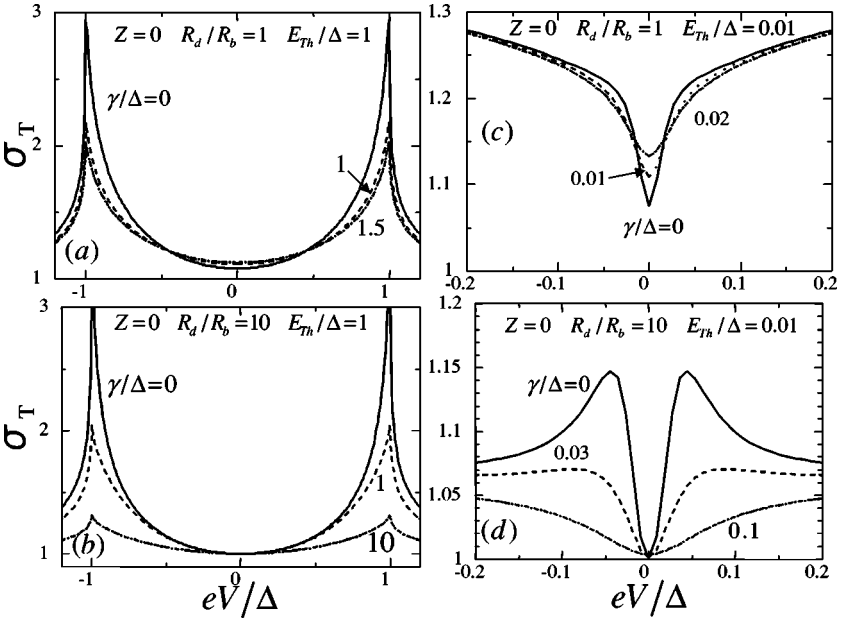

FIG. 4. Normalized conductance for high transparent junctions with $Z=0$.

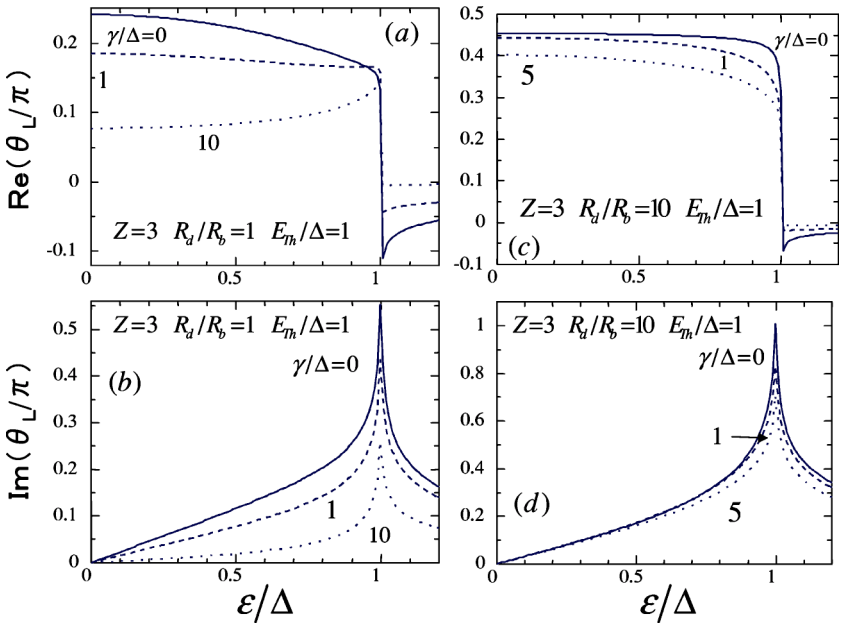

FIG. 5. Real (upper panels) and imaginary (lower panels) part of θ_L for $Z=3$ and $E_{\mathrm{Th}}/\Delta=1$.

seen from these figures, the characteristic energy range of γ which modifies the magnitude of σ_T(eV), is determined by E_{Th}, in agreement with the previous study based on the KL boundary conditions.[27]

In the case of an intermediate barrier strength $Z=1$ (Fig. 3) the magnitude of σ_T(eV) always exceeds unity. The resulting line shapes of σ_T(eV) for $E_{\mathrm{Th}}/\Delta=1$ are quite similar to the corresponding curves for $Z=3$ [see Figs. 3(a) and 3(b)]. For $E_{\mathrm{Th}}/\Delta=1$ and $R_d/R_b=1$, the zero-bias value $\sigma_T(0)$ is independent of γ/Δ [see Fig. 3(a)], in contrast to the corresponding case shown in Fig. 2(a). Another important difference from the case of large Z-factor is the absence of ZBCP for low Thouless energy. It is seen that for $E_{\mathrm{Th}}/\Delta=0.01$ a ZBCD occurs in both cases of $R_d/R_b=1$ and $R_d/R_b=10$. This conductance dip and the finite voltage peaks are fully suppressed with the increase of γ/Δ for $R_d/R_b=1$ [see Fig. 3(c)]. On the other hand, for $R_d/R_b=10$ only the peaks around $\mathrm{eV}/\Delta\sim0.04$ are suppressed while the magnitude of $\sigma(0)$ does not depend on γ, similar to the case $Z=3$ [see Fig. 3(d)]. The relevant scale of γ is again given by the magnitude of E_{Th}.

For the fully transparent case with $Z=0$ (Fig. 4), σ_T(eV) also always exceeds unity. The line shapes of σ_T(eV) with $E_{\mathrm{Th}}/\Delta=1$ are similar to the corresponding curves for $Z=3$ and $Z=1$ [see Figs. 4(a) and 4(b)]. For $E_{\mathrm{Th}}/\Delta=1$ and $R_d/R_b=1$, the magnitude of $\sigma_T(0)$ is enhanced by γ/Δ in contrast to the corresponding cases shown in Figs. 2(a) and 3(a) [see Fig. 4(a)]. For $E_{\mathrm{Th}}/\Delta=0.01$ and $R_d/R_b=1$, σ_T(eV) has a ZBCD. The magnitude of $\sigma_T(0)$ is enhanced by γ/Δ and the depth of the ZBCD decreases with the increase of γ/Δ [see Fig. 4(c)]. On the other hand, for $E_{\mathrm{Th}}/\Delta=0.01$ and $R_d/R_b=10$, the magnitude of $\sigma(0)$ does not depend on γ while the finite bias peaks are suppressed similar to the cases of $Z=3$ and $Z=1$ [see Fig. 4(d)].

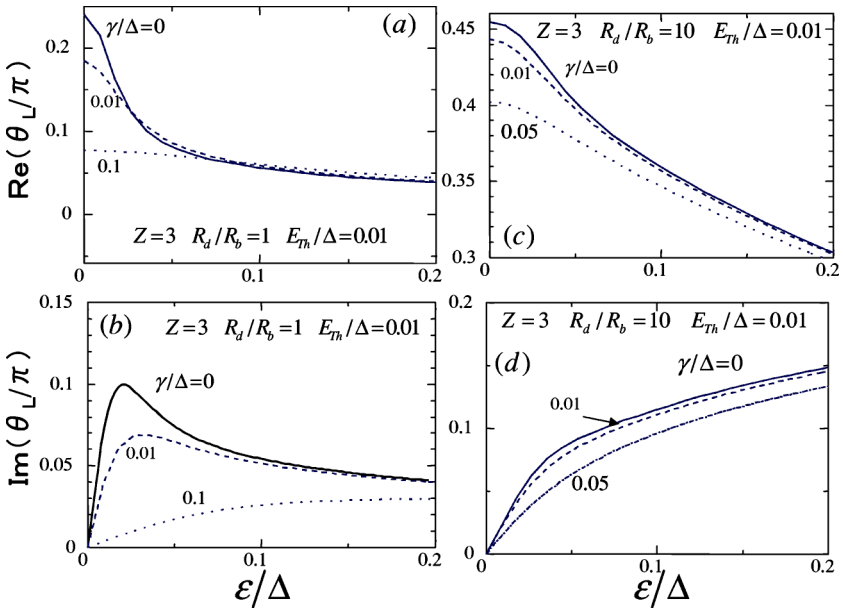

FIG. 6. Real (upper panels) and imaginary (lower panels) part of θ_L for $Z=3$ and $E_{\mathrm{Th}}/\Delta=0.01$.

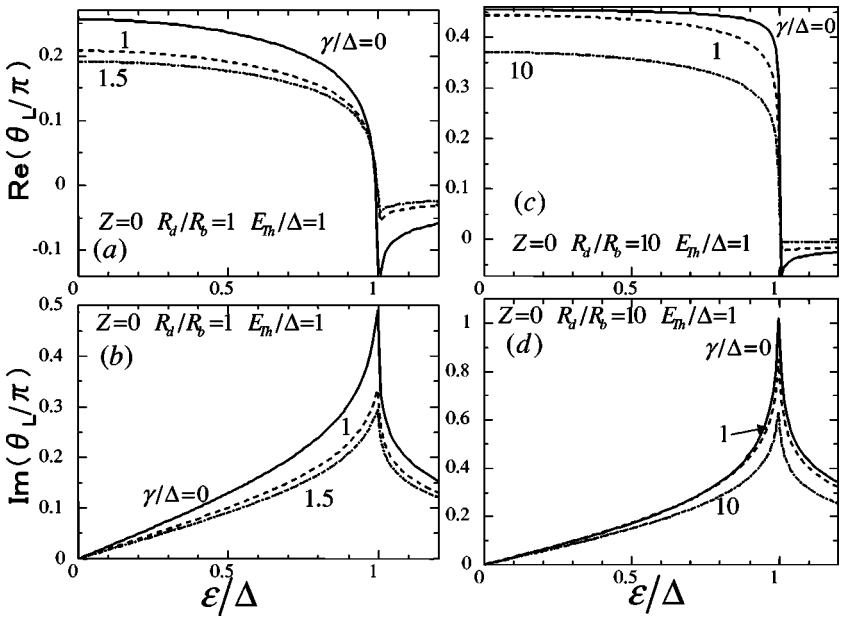

FIG. 7. Real (upper panels) and imaginary (lower panels) parts of θ_L for high transparent junctions with $Z=0$ and $E_{\mathrm{Th}}/\Delta=1$.

In order to understand the above wide variety of line shapes and their relation to the proximity effect, we shall discuss the behavior of function θ_L which is the measure of the proximity effect at the DN/S interface and determines the normalized local density of states by Re cos $\theta(x)$. At $\epsilon=0$, θ_L is always a real number even for nonzero γ. First, we study the case of $Z=3$ and $E_{\mathrm{Th}}/\Delta=1$ (Fig. 5) where the same values of γ/Δ and R_d/R_b are chosen as in Fig. 2. The real part of θ_L has a step-function-like structure and it is always positive for $\epsilon \leqslant \Delta$ and negative otherwise. The absolute value of the real part of θ_L decreases with an increase in γ/Δ. At the same time, the imaginary part of θ_L has a coherent peak, the height of which is reduced with an increase in γ/Δ. For the case of $Z=3$ and $E_{\mathrm{Th}}/\Delta=0.01$ (Fig. 6) where the same values of γ/Δ are chosen as in Fig. 2, the real part of θ_L has a ZBCP with the width given by E_{Th}. The imaginary part of θ_L has a ZBCD for $R_d/R_b=1$. Both the amplitudes of the real and imaginary part of θ_L are reduced with the increase of γ/Δ only around zero energy in the interval of the order of E_{Th}.

Next we consider the case of $Z=0$ with $E_{\mathrm{Th}}/\Delta=1$ (Fig. 7) and $E_{\mathrm{Th}}/\Delta=0.01$ (Fig. 8) where the same values of γ/Δ are chosen as in Fig. 4. The line shapes of both Re(θ_L) and Im(θ_L) are similar to those in Figs. 5 and 6. There is no clear qualitative difference between the energy dependencies of Real[Imag](θ_L) for $Z=0$ and those for $Z=3$. For all cases, the magnitude of θ_L is reduced with the increase of γ and then the proximity effect is suppressed by the magnetic impurity scattering within the energy range determined by E_{Th}. In almost all cases, the magnitude of σ_T(eV) is reduced with the decrease of θ_L. Only for the high transparent case with not so large R_d/R_b, the decrease of the magnitude of θ_L, i.e., the reduction of the proximity effect, can enhance the magnitude of σ_T(eV).

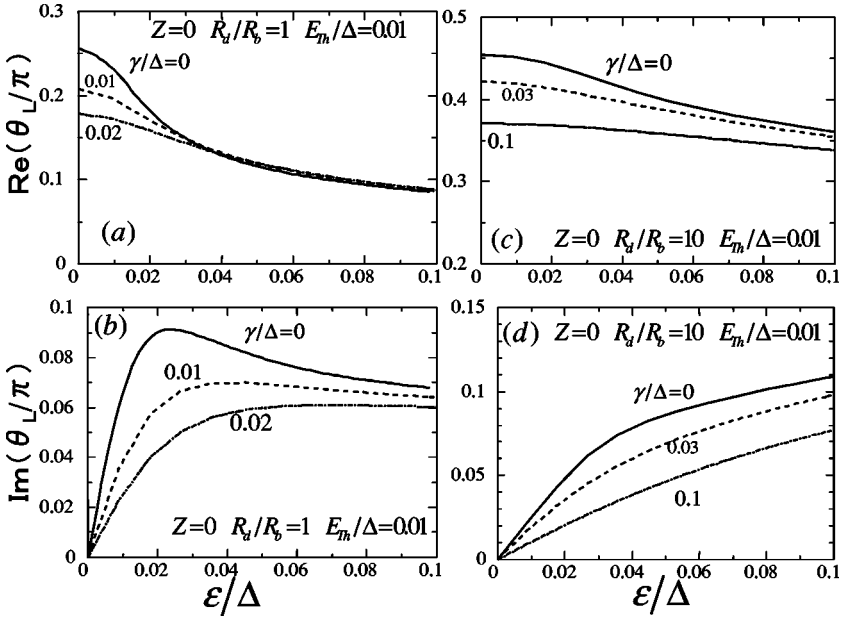

FIG. 8. Real (upper panels) and imaginary (lower panels) parts of θ_L for high transparent junctions with $Z=0$ and $E_{\mathrm{Th}}/\Delta=0.01$.

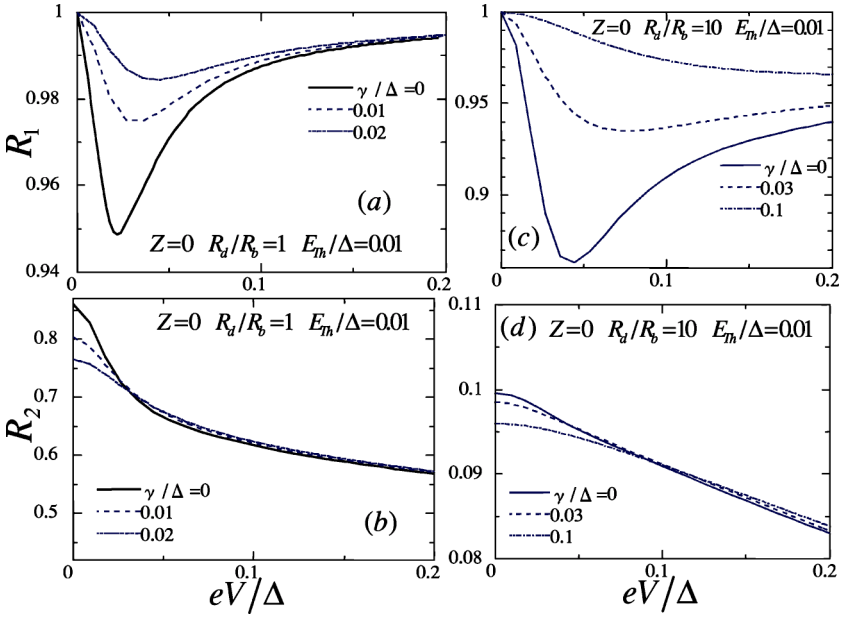

FIG. 9. Normalized resistance for $Z=0$ and $E_{\mathrm{Th}}/\Delta=0.01$.

In the following, we explain the wide variety of the line shapes of σ_T(eV). We consider $Z=0$ and $E_{\mathrm{Th}}/\Delta=1$ case, where θ_L has a weak energy dependence around zero voltage. For the fully transparent case with $T_m=1$, i.e., $Z=0$, $\sigma_T(0)$ can be given by

$$\sigma_T(0)=\frac{1+R_d/R_b}{1/\langle I_{b0}\rangle+R_d/R_b}. \tag{7}$$

with

$$\langle I_{b0}\rangle=\frac{2}{1+\sin\theta_L}. \tag{8}$$

From this equation we find that the magnitude of $\sigma_T(0)$ gets close to unity under the strong proximity effect, i.e., when the magnitude of R_d/R_b is large. As shown in Figs. 7(a) and 7(b), the magnitude of θ_L at $\epsilon=0$ is lowered with an increase in γ/Δ for $R_d/R_b=1$. Then, according to Eqs. (7) and (8), the resulting σ_T(eV) around eV$\sim$0 is slightly enhanced as shown in Fig. 4(a). For $R_d/R_b=10$, the magnitude of R_d/R_b is much larger than the magnitude of $1/\langle I_{b0}\rangle$. Then the γ dependence of $\sigma_T(0)$ becomes negligible as shown in Fig. 4(b). In order to understand the case of $Z=0$ and the small magnitude of E_{Th}/Δ, we decompose R into R_1 and R_2 following the previous work,[37] where R_1 and R_2 are defined by

$$R_1=\frac{1}{L}\int_0^L\frac{dx}{\cosh^2\theta_{im}(x)}$$

and

$$R_2=\frac{R_b}{R_d\langle I_{b0}\rangle}.$$

Figure 9 shows that R_1 has a minimum at a finite voltage which can result in a ZBCD and that R_2 has a maximum for high transparent junctions. For a large magnitude of R_d/R_b, the effect of R_1 is dominant, then the normalized conductance always has a ZBCD [see Figs. 9(c), 9(d), and 4(d)]. Since R_2 has a maximum at zero voltage [Fig. 9(b)], the resulting σ_T(eV) has a ZBCD as shown in Fig. 4(c).

Next we focus on the zero voltage resistance R/R_b as a function of R_d/R_b. For $Z=3$, R/R_b has a reentrant behavior as a function of R_d/R_b due to the so-called reflectionless

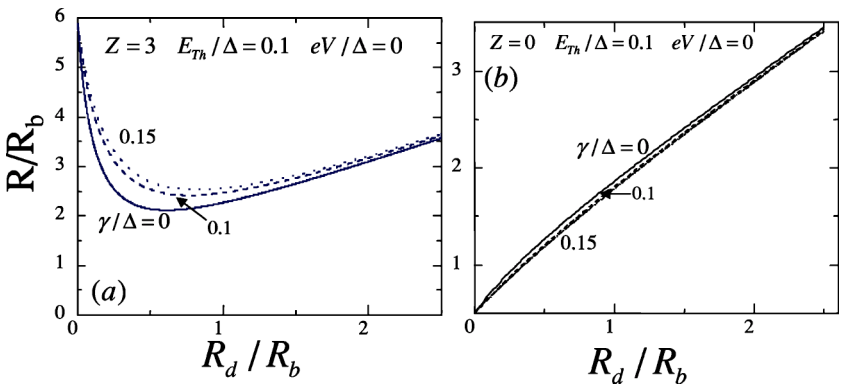

FIG. 10. Normalized zero voltage resistance as a function of R_d/R_b.

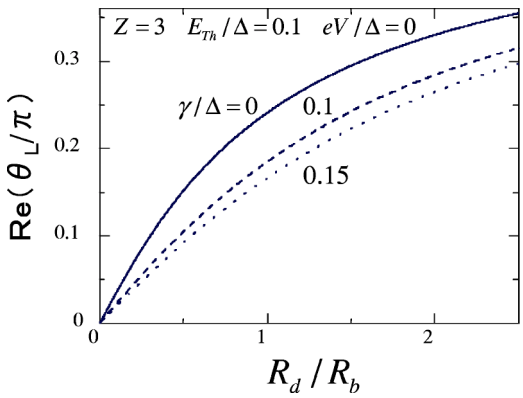

FIG. 11. Real part of θ_L at zero energy as a function of R_d/R_b.

tunneling effect[20] [see Fig. 10(a)]. With the increase of γ, this effect is smeared since the magnitude of θ_L is reduced as shown in Fig. 11. In contrast, for $Z=0$, where R/R_b increases monotonically as a function of R_d/R_b, the γ dependence of R/R_b is very weak [see Fig. 10(b)].

B. Tunneling conductance for *d*-wave junctions

Below we discuss the results of calculations for the *d*-wave case. Figure 12 shows the normalized conductance for $Z=10$, $R_d/R_b=1$, $E_{\mathrm{Th}}/\Delta=0.01$, and $\alpha/\pi=0$ where α denotes the misorientation angle between the normal to the interface and the crystal axis of *d*-wave superconductors. In this case, MARS are not formed at the interface of the *d*-wave superconductor. The origin of the ZBCP is due to the proximity effect in the DN region and the height of the ZBCP is suppressed with increasing γ similar to the case of the *s*-wave junctions.

With the increase of the magnitude of α the MARS are formed at the interface. The MARS contribute to the charge transport across the junction and leads to the formation of the ZBCP. As is seen in Fig. 13, the ZBCP does not depend on γ for $Z=10$, $R_d/R_b=1$, $E_{\mathrm{Th}}/\Delta=0.01$, and $\alpha/\pi=0.125$. The similar result is obtained for different angle $\alpha/\pi=0.25$. The reason is that MARS reduce the proximity effect in DN,

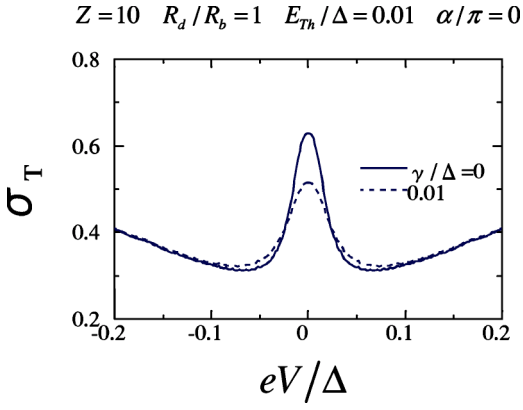

FIG. 12. Normalized conductance in a *d*-wave junction for $Z=10$, $R_d/R_b=1$, $E_{\mathrm{Th}}/\Delta=0.01$, and $\alpha/\pi=0$.

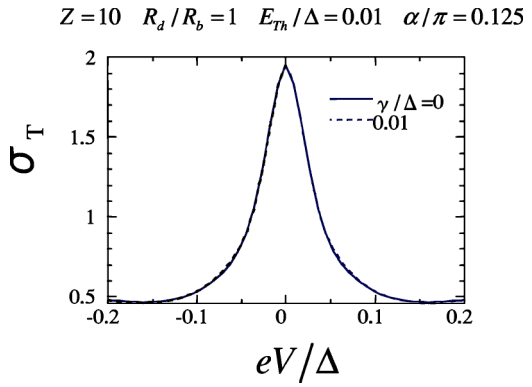

FIG. 13. Normalized conductance in a *d*-wave junction for $Z=10$, $R_d/R_b=1$, $E_{\mathrm{Th}}/\Delta=0.01$, and $\alpha/\pi=0.125$.

therefore the influence of magnetic impurity scattering on the σ_T becomes less important. In the extreme case, $\alpha=0.25\pi$, the proximity effect is completely absent by the symmetry of the pair potential and σ_T is completely independent of γ.

IV. CONCLUSIONS

We have performed a detailed theoretical study of the conductance of diffusive normal metal/*s*- and *d*-wave superconductor junctions in the presence of magnetic impurities. Below, the main results obtained in this paper are summarized.

(1) For the *s*-wave junctions, the proximity effect is suppressed by the magnetic impurity scattering within the energy range determined by the Thouless energy in DN. In this range both the real and imaginary parts of the proximity effect parameter, i.e., $\mathrm{Re}(\theta_L)$ and $\mathrm{Im}(\theta_L)$ are reduced with the increase of the magnitude of γ for any transparency of the insulating barrier.

(2) The magnitude of the normalized bias voltage dependent conductance $\sigma_T(\mathrm{eV})$ in the low transparent *s*-wave junctions is suppressed by the magnetic impurity scattering. On the other hand, for high transparent *s*-wave junctions, $\sigma_T(\mathrm{eV})$ can be enhanced by the magnetic impurity scattering.

(3) In the *d*-wave junctions, the zero bias conductance peak formed for low transparent barriers is suppressed by the magnetic impurity scattering only for $\alpha\sim 0$. For other misorientation angles the conductance is not sensitive to the magnetic impurity scattering in a diffusive normal metal.

In the present paper, we have discussed the case where magnetic impurities are located in DN. These results can be also applied to the situation when the junction is in a weak magnetic field H. If the field direction is parallel to the junction plane, the pair-breaking rate is given by $\gamma=e^2w^2DH^2/6$, where w is the transverse size of the DN.[35] Assuming $w=10^{-5}$ m, $D=10^{-2}$ m^2/s, $\Delta=10^{-3}$ eV, and $H=10^{-4}-10^{-2}$ T, we estimate the pair-breaking rate $\gamma/\Delta=10^{-3}\sim 10$. This range of γ corresponds to the parameters chosen in the present paper. The suppression of the

ZBCP and ZBCD by the magnetic field was actually observed in several experiments.[5,7,11–13,15] The results of the present paper may serve as a guide to study the charge transport in the junctions with magnetic impurities or under applied magnetic field.

It is also an interesting problem to study the influence of the magnetic impurity scattering on diffusive normal metal/triplet superconductor junctions where anomalous proximity effect is expected.[45] An application of the present theory to the S/N/S junctions with unconventional superconductors also requires separate investigation.

ACKNOWLEDGMENTS

The authors appreciate useful and fruitful discussions with Yu. Nazarov and H. Itoh. This work was supported by the Core Research for Evolutional Science and Technology (CREST) of the Japan Science and Technology Corporation (JST) and a Grant-in-Aid for the 21st Century COE "Frontiers of Computational Science." The computational aspect of this work has been performed at the facilities of the Supercomputer Center, Institute for Solid State Physics, University of Tokyo and the Computer Center.

[1] A. F. Andreev, Sov. Phys. JETP **19**, 1228 (1964).
[2] G. E. Blonder, M. Tinkham, and T. M. Klapwijk, Phys. Rev. B **25**, 4515 (1982).
[3] A. V. Zaitsev, Sov. Phys. JETP **59**, 1163 (1984).
[4] F. W. J. Hekking and Yu. V. Nazarov, Phys. Rev. Lett. **71**, 1625 (1993).
[5] F. Giazotto, P. Pingue, F. Beltram, M. Lazzarino, D. Orani, S. Rubini, and A. Franciosi, Phys. Rev. Lett. **87**, 216808 (2001).
[6] T. M. Klapwijk, Physica B **197**, 481 (1994).
[7] A. Kastalsky, A. W. Kleinsasser, L. H. Greene, R. Bhat, F. P. Milliken, and J. P. Harbison, Phys. Rev. Lett. **67**, 3026 (1991).
[8] C. Nguyen, H. Kroemer, and E. L. Hu, Phys. Rev. Lett. **69**, 2847 (1992).
[9] B. J. van Wees, P. de Vries, P. Magnee, and T. M. Klapwijk, Phys. Rev. Lett. **69**, 510 (1992).
[10] J. Nitta, T. Akazaki, and H. Takayanagi, Phys. Rev. B **49**, 3659 (1994).
[11] S. J. M. Bakker, E. van der Drift, T. M. Klapwijk, H. M. Jaeger, and S. Radelaar, Phys. Rev. B **49**, 13275 (1994).
[12] P. Xiong, G. Xiao, and R. B. Laibowitz, Phys. Rev. Lett. **71**, 1907 (1993).
[13] P. H. C. Magnee, N. van der Post, P. H. M. Kooistra, B. J. van Wees, and T. M. Klapwijk, Phys. Rev. B **50**, 4594 (1994).
[14] J. Kutchinsky, R. Taboryski, T. Clausen, C. B. Sorensen, A. Kristensen, P. E. Lindelof, J. Bindslev Hansen, C. Schelde Jacobsen, and J. L. Skov, Phys. Rev. Lett. **78**, 931 (1997).
[15] W. Poirier, D. Mailly, and M. Sanquer, Phys. Rev. Lett. **79**, 2105 (1997).
[16] C. W. J. Beenakker, Rev. Mod. Phys. **69**, 731 (1997).
[17] C. J. Lambert, J. Phys.: Condens. Matter **3**, 6579 (1991).
[18] Y. Takane and H. Ebisawa, J. Phys. Soc. Jpn. **61**, 2858 (1992).
[19] C. W. J. Beenakker, Phys. Rev. B **46**, 12841 (1992).
[20] C. W. J. Beenakker, B. Rejaei, and J. A. Melsen, Phys. Rev. Lett. **72**, 2470 (1994).
[21] G. B. Lesovik, A. L. Fauchere, and G. Blatter, Phys. Rev. B **55**, 3146 (1997).
[22] A. F. Volkov, A. V. Zaitsev, and T. M. Klapwijk, Physica C **210**, 21 (1993).
[23] K. D. Usadel, Phys. Rev. Lett. **25**, 507 (1970).
[24] M. Yu. Kupriyanov and V. F. Lukichev, Zh. Eksp. Teor. Fiz. **94**, 139 (1988) [Sov. Phys. JETP **67**, 1163 (1988].
[25] Yu. V. Nazarov, Phys. Rev. Lett. **73**, 1420 (1994).
[26] S. Yip, Phys. Rev. B **52**, 3087 (1995).
[27] S. Yip, Phys. Rev. B **52**, 15504 (1995).
[28] Yu. V. Nazarov and T. H. Stoof, Phys. Rev. Lett. **76**, 823 (1996); T. H. Stoof and Yu. V. Nazarov, Phys. Rev. B **53**, 14496 (1996).
[29] A. F. Volkov, N. Allsopp, and C. J. Lambert, J. Phys.: Condens. Matter **8**, L45 (1996); A. F. Volkov and H. Takayanagi, Phys. Rev. B **56**, 11184 (1997).
[30] A. A. Golubov, F. K. Wilhelm, and A. D. Zaikin, Phys. Rev. B **55**, 1123 (1997).
[31] A. F. Volkov and H. Takayanagi, Phys. Rev. B **56**, 11184 (1997).
[32] E. V. Bezuglyi, E. N. Bratus', V. S. Shumeiko, G. Wendin, and H. Takayanagi, Phys. Rev. B **62**, 14439 (2000).
[33] R. Seviour and A. F. Volkov, Phys. Rev. B **61**, R9273 (2000).
[34] W. Belzig *et al.*, Superlattices Microstruct. **25**, 1251 (1999).
[35] W. Belzig, C. Bruder, and G. Schön, Phys. Rev. B **54**, 9443 (1996).
[36] Yu. V. Nazarov, Superlattices Microstruct. **25**, 1221 (1999); cond-mat/9811155 (unpublished).
[37] Y. Tanaka, A. A. Golubov, and S. Kashiwaya, Phys. Rev. B **68**, 054513 (2003).
[38] L. J. Buchholtz and G. Zwicknagl, Phys. Rev. B **23**, 5788 (1981); C. Bruder, *ibid.* **41**, 4017 (1990); C. R. Hu, Phys. Rev. Lett. **72**, 1526 (1994).
[39] Y. Tanaka and S. Kashiwaya, Phys. Rev. Lett. **74**, 3451 (1995); S. Kashiwaya, Y. Tanaka, M. Koyanagi, and K. Kajimura, Phys. Rev. B **53**, 2667 (1996); Y. Tanuma, Y. Tanaka, and S. Kashiwaya, *ibid.* **64**, 214519 (2001); Y. Asano, Y. Tanaka, and S. Kashiwaya, *ibid.* **69**, 134501 (2004).
[40] S. Kashiwaya and Y. Tanaka, Rep. Prog. Phys. **63**, 1641 (2000), and references therein.
[41] L. Alff, H. Takashima, S. Kashiwaya, N. Terada, H. Ihara, Y. Tanaka, M. Koyanagi, and K. Kajimura, Phys. Rev. B **55**, R14757 (1997); M. Covington, M. Aprili, E. Paraoanu, L. H. Greene, F. Xu, J. Zhu, and C. A. Mirkin, Phys. Rev. Lett. **79**, 277 (1997); J. Y. T. Wei, N.-C. Yeh, D. F. Garrigus, and M. Strasik, *ibid.* **81**, 2542 (1998).
[42] H. Kashiwaya, I. Kurosawa, S. Kashiwaya, A. Sawa, and Y. Tanaka, Phys. Rev. B **68**, 054527 (2003); H. Kashiwaya, S. Kashiwaya, B. Prijamboedi, A. Sawa, I. Kurosawa, Y. Tanaka, and I. Iguchi, *ibid.* **70**, 094501 (2004).
[43] Y. Tanaka, Y. V. Nazarov, and S. Kashiwaya, Phys. Rev. Lett. **90**, 167003 (2003).
[44] Y. Tanaka, Y. V. Nazarov, A. A. Golubov, and S. Kashiwaya, Phys. Rev. B **69**, 144519 (2004).
[45] Y. Tanaka and S. Kashiwaya, Phys. Rev. B **69**, 012507 (2004).